Nano-Preciptates Design with Hydrogen Trapping Character in High Strength Steel

Fu-Gao Wei, Toru Hara, and Kaneaki Tsuzaki

Abstract

Nano-precipitates of alloy carbides TiC, NbC and VC which have the same NaCl-type crystal structure in tempered martensite have been characterized by means of high-resolution transmission electron microscope (HRTEM) and correlated to the hydrogen trapping property. The examination of whether the amount of hydrogen absorbed by the TiC particles depends on their surface area or volume indicate that the coherent and semi-coherent TiC particles trap hydrogen at the precipitate/matrix interface at ambient temperature while the incoherent TiC particles trap hydrogen inside themselves only at high temperatures. Coherent and semi-coherent NbC and VC particles also demonstrate a surface area dependence of hydrogen trapping capacity with NbC > TiC ≫ VC. Contrary to TiC, incoherent NbC and VC particles are unable to trap hydrogen.

Keywords

High strength steel • Hydrogen embrittlement • MX carbide • HRTEM • Thermal desorption spectrometry

1 Introduction

Titanium carbide has been known to have a strong interaction with hydrogen through the electrochemical permeation method [1] and the thermal desorption spectrometry (TDS) analysis [2, 3]. The activation energy for the desorption of hydrogen from TiC precipitates in steels was estimated to be as high as 95 [1] or 87 kJ/mol [2].

Our recent study also showed high activation energy for TiC particles [4]. However, these results only seemed to be valid for incoherent TiC particles. The coherent or semi-coherent TiC particles in the 0.42C-0.30Ti steel demonstrated a different hydrogen trapping characteristic; the activation energy is much lower than that for the incoherent particles [5]. Pressouyre and Bernstein [1, 6] pointed out earlier that the TiC particle becomes more reversible when its coherency with the matrix is increased; however, no experimental evidence has been provided. On the other hand, an autoradiography imaging of hydrogen [7] suggested that hydrogen is trapped at the precipitate/matrix interface. Thus, the first purpose of the present study is to investigate the relationship between the size and coherency of the TiC precipitate and its hydrogen trapping property. The first step is to produce a series of TiC precipitates of various interfacial characters ranging from coherent through semi-coherent to incoherent by heat treatment. The second step is to characterize these precipitates on an atomic scale; however, this was not possible due to the strong magnetism interference of low-alloy ferritic or martensitic steel. The third step is to

This article was originally published in "Effects of Hydrogen on Materials", ASM International, ISBN-13: 978-1-61503-003-3, (2009), pp. 448–455.

F.-G. Wei (✉)
Technology Development Department, Yakin Kawasaki Co., Ltd., 4-2 Kojima-cho, Kawasaki-ku, Kawasaki, Kanagawa 210-8558, Japan
e-mail: fugao.wei@nyk.jp

T. Hara · K. Tsuzaki
Structural Metals Center, National Institute for Materials Science, 1-2-1 Sengen, Tsukuba, Ibaraki 305-0047, Japan

Y. Weng et al. (eds.), *Advanced Steels*, DOI: 10.1007/978-3-642-17665-4_11,

correlate the size and coherency of the TiC precipitate to its hydrogen trapping property with an emphasis of obtaining the answer to the two questions: (1) how does the hydrogen trapping characteristic change with a successive variation of interfacial character from coherent to incoherent, and (2) does the amount of hydrogen trapped by (semi-)coherent and incoherent TiC precipitates depend on their surface area or volume? The answer to the second question determines the trap sites of hydrogen to be the precipitate/matrix interface or to be inside the precipitate.

The second purpose of the study is to investigate the hydrogen trapping properties of NbC and VC precipitates which have the same crystal structure as that of TiC. NbC and VC, along with TiC, are important carbides for microstructural control in microalloyed steels and low-alloy high strength steels. However, little is known regarding their hydrogen trapping properties. Thus, they are examined with an emphasis on comparing them to the TiC precipitate.

2 Experimental Method

Three steels containing equal molar fractions of TiC, NbC and VC, respectively, i.e. 0.05C-0.20Ti-2.0Ni, 0.05C-0.41Nb-2.0Ni and 0.05C-0.24V-2.0Ni in mass% were prepared. They were received in the form of hot-rolled plates that contained carbide precipitates in the ferrite matrix. The conditions of heat treatment, hydrogen charging and TDS analysis of the present steels were the same as those for the 0.05C-0.20Ti-2.0Ni steel in the previous study [8]. The major conditions are: (1) quenching from 1,350 C and tempering at 300 ~ 1,000 °C for 3 h, (2) dimension of the specimen for TDS analysis being ϕ5 mm × 40 mm, (3) cathodic charging of hydrogen in a 3 mass% NaCl + 0.3 mass% NH_4SCN) aqueous solution at a current density of 1 A/m^2 for a short time of 1 h to investigate the deep traps associated with TiC precipitates, (4) hydrogen analysis by TDS at a heating rate of 100 °C/h, (5) estimation of the activation energy for hydrogen desorption from traps by fitting the experimentally measured desorption spectrum to the Kissinger's first-order reaction kinetic formula, and (6) microstructural observation by means of HRTEM. The tempering temperature for NbC- and VC-containing steels was limited to 700 °C and the hydrogen charging time was extended to 48 h until the saturation of hydrogen entry.

3 Results and Discussion

3.1 Microstructural Characterization of TiC Precipitates on the Atomic Scale

Austenitization at 1,350°C dissolved all the TiC particles in austenite. Then a fully martensitic microstructure was produced by the quenching that followed. Tempering at 300–1,100°C after the quenching produced a series of TiC precipitates with interfacial characters changing from coherent to incoherent as expected. No precipitates other than TiC were observed. TiC began to precipitate at 500°C as a coherent precipitate and changed to semi-coherent particles at about 550°C. The semi-coherent character existed to 800°C beyond which it lost its coherency with the matrix. Coherent and semi-coherent TiC precipitates exhibit a disk-like shape with its broad face on the {100} planes of ferrite and satisfies the Baker–Nutting orientation relationship with the ferrite, i.e. $(100)_{TiC}//(100)_{\alpha}$, $[011]_{TiC}//[001]_{\alpha}$. A TiC precipitate in the 0.05C-0.20Ti-2.0Ni steel which was tempered at 600°C is shown in Fig. 1. The imaging process of the HRTEM micrograph revealed that there are misfit dislocations on the broad faces of the precipitate and the side faces as well [9]. The change in the size and shape of the TiC precipitate with tempering temperature is summarized in Fig. 2. Both the diameter and the thickness of the disc-like (semi-)coherent TiC precipitate increase with increasing tempering temperature with an abnormal increase at 800°C. Incoherent TiC precipitates formed above 800°C were observed to be approximately spherical.

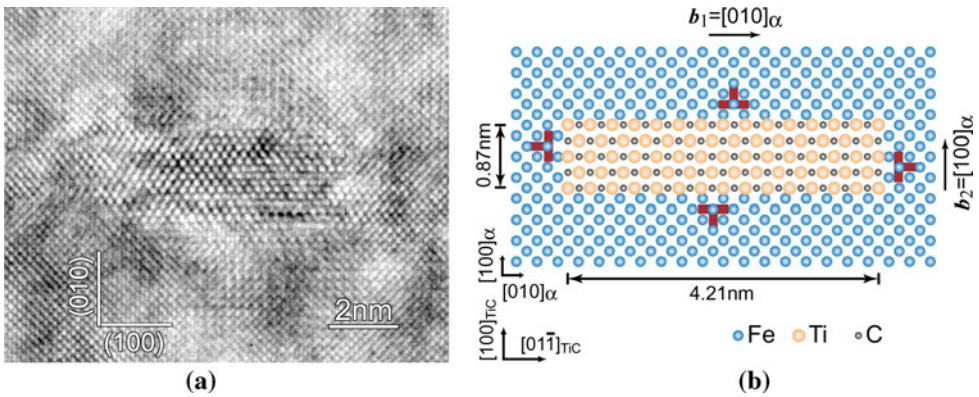

Fig. 1 Semi-coherent TiC precipitate in the 0.05C-0.20Ti-2.0Ni steel tempered at 600°C. **a** HRTEM micrograph and **b** schematic illustration of the lattice mismatch

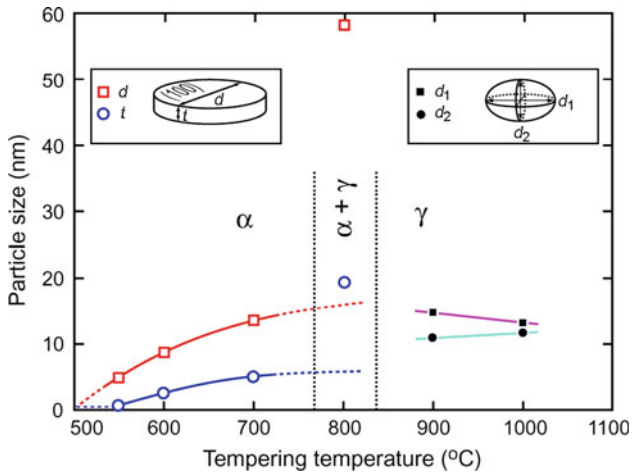

Fig. 2 Change in size and shape of TiC precipitate in the 0.05C-0.20Ti-2.0Ni steel with tempering temperature

3.2 Hydrogen Trapping of TiC Precipitates with Interfacial Characters from Coherent to Incoherent

The results of the TDS analysis on samples tempered at 300–1,100°C are shown in Fig. 3. A short hydrogen charging time of 1 h was selected for detecting the deepest trap associated with the TiC precipitates. Only a small peak at about 120°C is present for the samples that were tempered below 500°C. However, the desorption peak becomes larger and shifts to about 230°C when tempered at 500°C. On tempering above 550°C, the 230°C peak splits into two peaks; one remains at 230°C and the other (the subsidiary peak) shifts towards a high temperature as the tempering temperature increases. The 230°C peak becomes smaller when the tempering temperature increases and disappears in the spectrum of the sample that was tempered at 1,000°C.

The peak located at 120°C supposedly resulted from the hydrogen trapped by the grain boundaries and dislocations in the martensitic matrix [8]. The 230°C desorption peak was contributed from the hydrogen that was trapped by the broad face of the disc-shaped TiC precipitate. The subsidiary peak that split from the 230°C peak is from the side face of the precipitate. The hydrogen desorption activation energy deduced from the 230°C peak was about 55.8 kJ/mol for the samples that were tempered from 600 to 800°C. By dividing the hydrogen content by the total surface area of the broad faces, the hydrogen trapped by the broad faces of the disk-like semi-coherent TiC precipitate was estimated to be constant and about 1.3 atoms/nm^2 (Fig. 4). The facts of the constant hydrogen content per unit surface area and the constant desorption activation energy of relatively high values over the range of the tempering temperature of 600–800°C strongly suggest that hydrogen associated with the 230 °C peak is trapped at the same deep site on the broad face of the semi-coherent TiC precipitate. The deep site is probably the core of misfit dislocations as shown in Fig. 1b. This result implies that the higher the misfit dislocation density, the more the hydrogen will be trapped at the precipitate/matrix interface. The NbC is predicted to trap more hydrogen than TiC while VC will trap less hydrogen than TiC because NbC and VC show a higher and a lower lattice mismatch with the ferrite matrix than TiC, respectively. Another prediction is that hydrogen is likely to occupy the less distorted sites other than the misfit dislocation core on the interface when more hydrogen is charged into the steels.

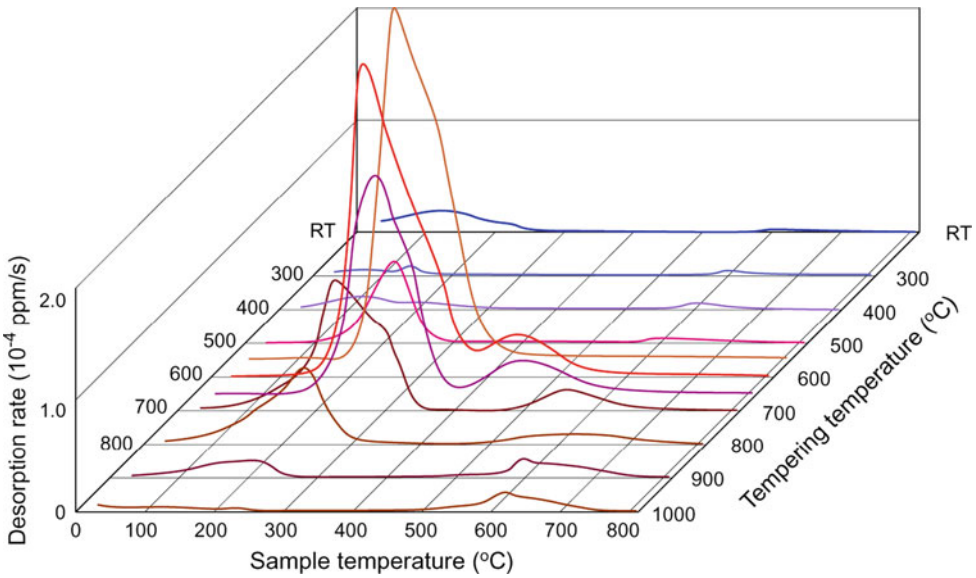

Fig. 3 Evolution of the TDS spectrum of the 0.05C-0.20Ti-2.0Ni steel quenched and tempered at various temperatures. Hydrogen charging time 1 h

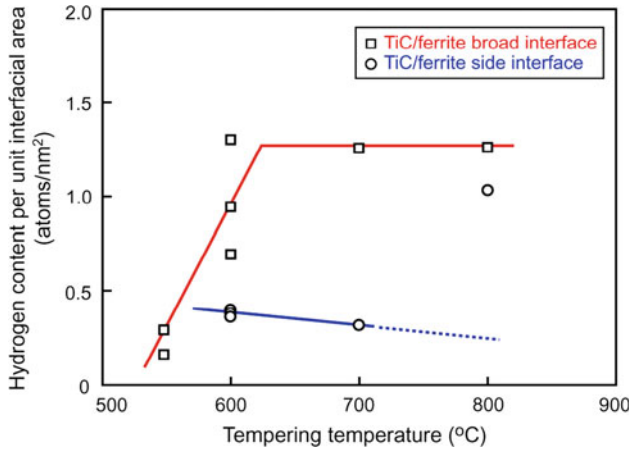

Fig. 4 The hydrogen trapped by the unit area of the broad and the side faces of the semi-coherent TiC precipitate, respectively. Hydrogen charging time 1 h

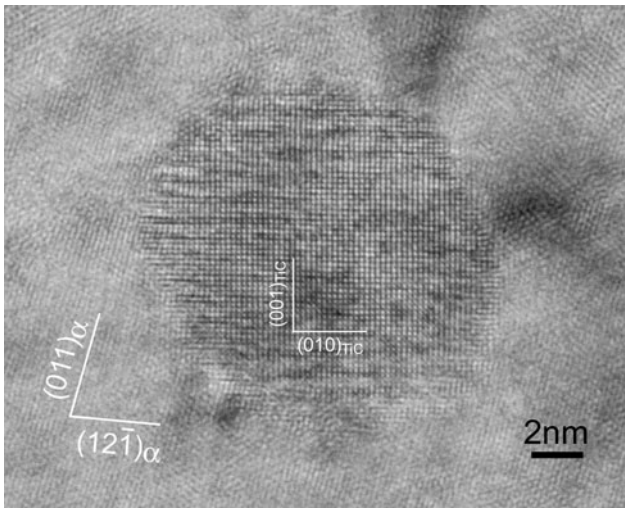

Fig. 5 An incoherent particle in the 0.05C-0.20Ti-2.0Ni steel

In contrast to the 230°C peak, the subsidiary desorption peak that is separated from it cannot be rationalized by the constant hydrogen content per unit surface area as shown in Fig. 4. The subsidiary desorption peak is interpreted to result from the hydrogen trapped at the carbon vacancy sites within the TiC precipitate beneath the side interface. The carbon vacancies are supposed to form during the Ostward ripening process of TiC precipitates during which the smaller particles begin to dissolve from the side face preferentially with a faster dissolution rate of carbon than titanium [10].

3.3 Hydrogen Trapping Characteristics of Incoherent TiC Particles

TiC particles have long been considered as a strong trap which can absorb hydrogen easily at ambient temperature. As described above, (semi-)coherent TiC precipitates are able to trap hydrogen easily during cathodic charging at room temperature. However, our recent study [11] found that incoherent TiC particles do not trap hydrogen at all at room temperature. Incoherent TiC can trap hydrogen but this is only possible at high temperatures. Figure 5 shows an incoherent TiC particle in the as-received 0.05C-0.20Ti-2.0Ni steel. The incoherent TiC particles that remained undissolved during austenitization absorb hydrogen from the environmental atmosphere. The hydrogen trapped by the incoherent TiC, which is characterized by a desorption peak at around 600°C, depends on the amount or more accurately the volume [8] of undissolved TiC particles (Fig. 6a). At room temperature, the incoherent TiC particles cannot be charged with hydrogen even with a long charging time and a

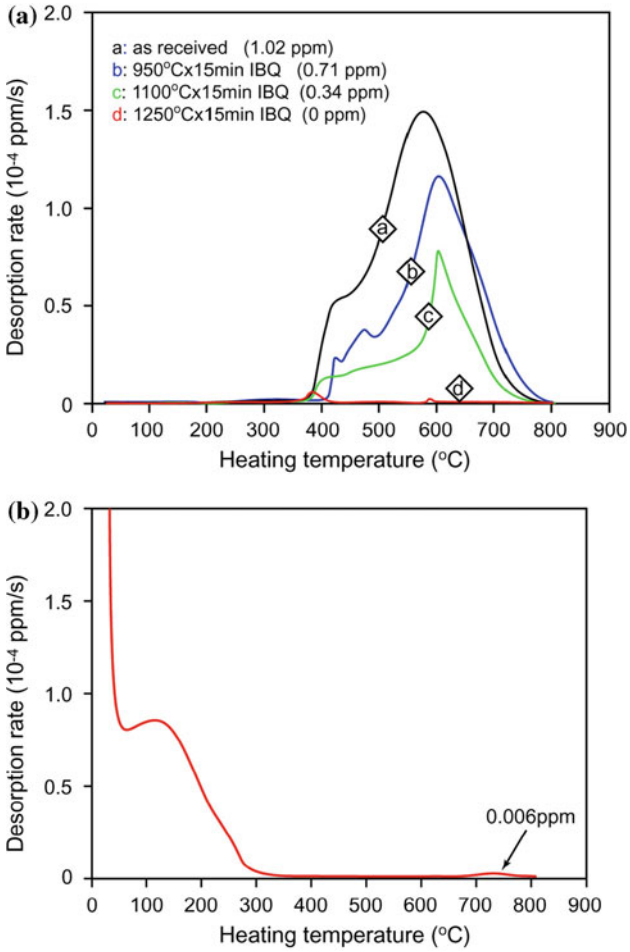

Fig. 6 TDS analysis of hydrogen trapped by incoherent TiC particles in the as-received 0.05C-0.20Ti-2.0Ni steel. **a** Analysis without cathodic charging after austenitization at various temperatures, and **b** analysis after vacuum degassing at 950°C and prolonged cathodic hydrogen charging at a high current density

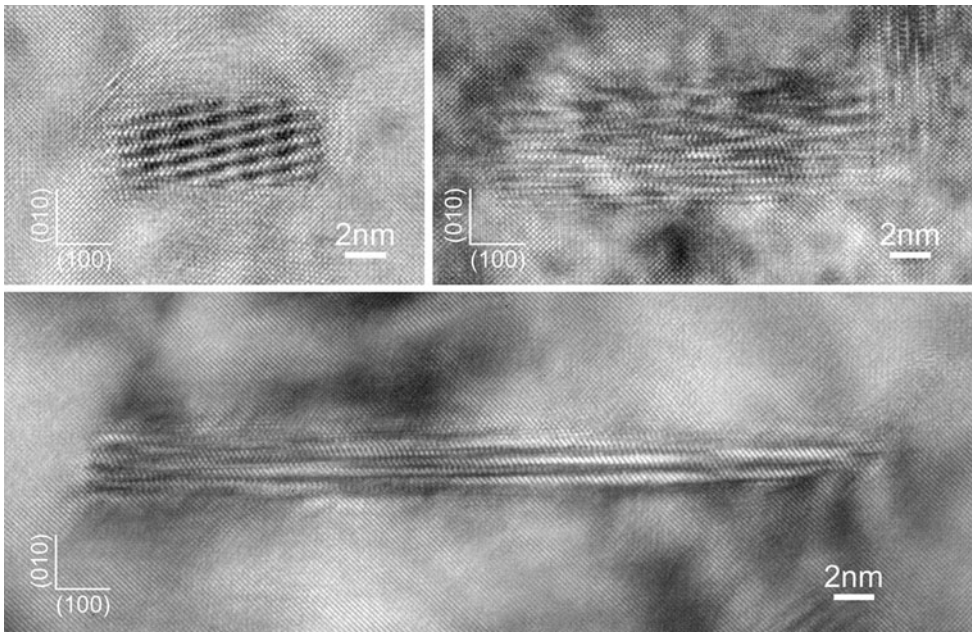

Fig. 7 HRTEM micrographs of NbC, TiC and VC precipitates in the 0.05C-0.41Nb-2.0Ni, 0.05C-0.20Ti-2.0Ni and 0.05C-0.24 V-2.0Ni steels quenched and tempered at 700°C, respectively

high current density (Fig. 6b). The inability of hydrogen trapping of incoherent TiC particles at low temperatures is explained by the trap site of carbon vacancies which requires high activation energy for both trapping and detrapping of hydrogen.

3.4 Hydrogen Trapping of NbC and VC Precipitates

NbC and VC nano-precipitates show a disk-like appearance like that of TiC and maintain the Baker–Nutting orientation relationship with ferrite. However, their diameters differ noticeably compared to that of TiC although they all have almost the same thickness (Fig. 7) [12]. The diameter of the disk-shaped carbide is proportional to the reciprocal of its lattice misfit (Fig. 8a), which means that there is the same number of misfit dislocations on the broad face of each particle if the same misfit dislocation configuration is assumed (Fig. 8b).

Figure 9 shows the TDS spectra obtained after hydrogen charging to saturation for the three steels tempered at 700°C containing the NbC, TiC and VC precipitates, respectively. Contrary to TiC, NbC and VC do not have a desorption peak at around 600°C. The reason for this difference has not been clarified yet. The precipitates contribute significantly to the desportion peaks below 250°C. The hydrogen trapping ability of the alloy carbides varies in the descending order of NbC > TiC ≫ VC. This finding shows a good agreement with the above prediction based on the density of misfit dislocations on the broad face of the disk-shaped alloy carbide precipitate.

The results obtained in this study emphasize that the hydrogen trapping property, i.e. hydrogen trapping capacity and the hydrogen–precipitate interaction energy, depends considerably on the type of alloy carbides, precipitate/ferrite interfacial character and the crystal defects within the precipitate. Composition selection and microstructural control of alloy carbides may offer a variety of options for the application of alloy carbides as hydrogen trap sites in the development of hydrogen embrittlement resistant steels.

Conclusions

(1) (Semi-)coherent TiC precipitates trap hydrogen at precipitate/ferrite interfaces. The core of misfit dislocations on the broad face of the disk-shaped precipitate is supposed to act as hydrogen trap sites at a low hydrogen concentration.
(2) Incoherent TiC particle is unable to trap hydrogen at ambient temperature. High temperatures are required for incoherent TiC particle to trap and detrap hydrogen. The carbon vacancies are probably the trap sites for hydrogen in incoherent TiC particles.

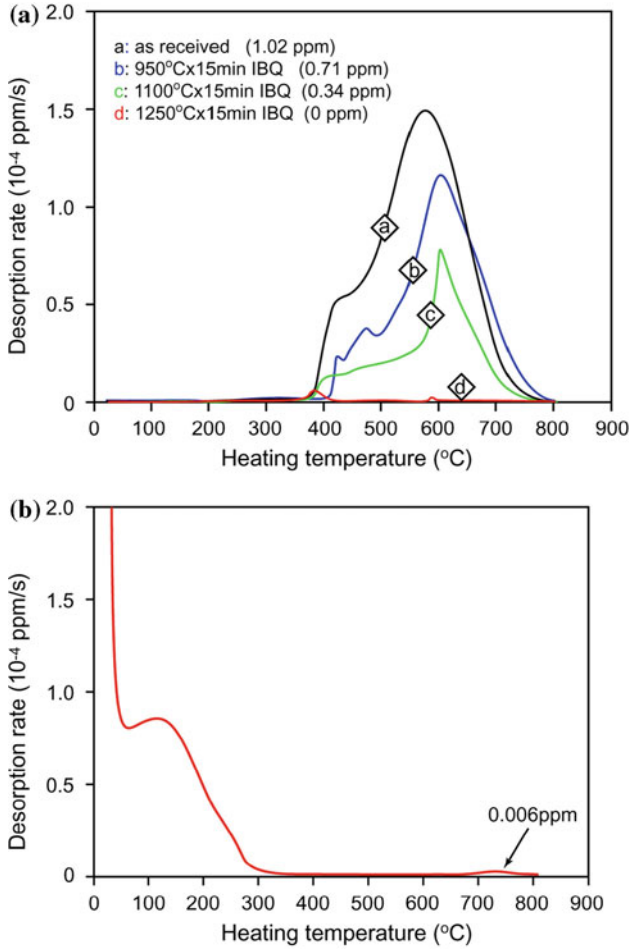

Fig. 8 Size and morphology of disk-like NbC, TiC and VC in the steels tempered at 700°C. **a** Relationship between diameter and lattice misfit, and **b** illustration of misfit dislocations on the broad faces of the precipitates

(3) The hydrogen trapping ability of (semi-)coherent alloy carbides varies in the descending order of NbC > TiC ≫ VC. Unlike TiC, neither NbC nor VC show any desorption peak at high temperatures around 600°C.

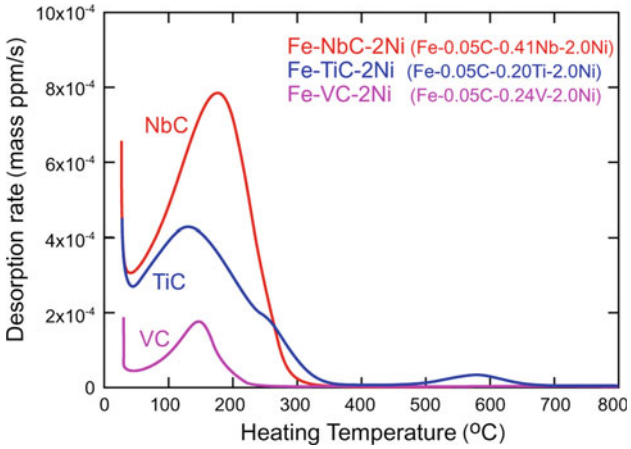

Fig. 9 TDS spectra for 0.05C-0.41Nb-2.0Ni, 0.05C-0.20Ti-2.0Ni and 0.05C-0.24V-2.0Ni steels quenched and tempered at 700°C. Charging time: 48 h

References

1. G.M. Pressouyre, I.M. Bernstein, Metall. Trans. A **9A**, 1571 (1978)
2. H.G. Lee, J.Y. Lee, Acta Metall. **32**, 131 (1984)
3. S.M. Lee, J.Y. Lee, Acta Metall. **35**, 2695 (1987)
4. F.G. Wei, T. Hara, K. Tsuzaki, Metall. Mater. Trans. B **35B**, 587 (2004)
5. F.G. Wei, T. Hara, T. Tsuchida, K. Tsuzaki, Iron Steel Inst. Jpn. Int. **43**, 539 (2003)
6. G.M. Pressouyre, I.M. Bernstein, Metall. Trans. A **10A**, 1571 (1979)
7. A. Asaoka, G. Lapasset, M. Aucouturier, P. Lacombe, Corrosion **34**, 39 (1978)
8. F.G. Wei, K. Tsuzaki, Metall. Mater. Trans. A**37A**, 331 (2006)
9. F.G. Wei, T. Hara, K. Tsuzaki, Phil. Mag. **84**, 1735 (2004)
10. F.G. Wei, T. Hara, K. Tsuzaki, Ferrum (Bull. Iron Steel Inst. Jpn.) **12**, 766 (2007)
11. F.G. Wei, K. Tsuzaki, Metall. Mater. Trans. A**35A**, 3155 (2004)
12. F.G. Wei, K. Tsuzaki, Second Place Award of International Metallographic Contest, Class 3: Electron Microscopy—Transmission and Analytical (2008), http://www.metallography.com/ims/contest.htm